AGU PUBLICATIONS

JGR

Journal of Geophysical Research: Space Physics

RESEARCH ARTICLE
10.1002/2014JA020813

Key Points:
- We study the long-term trends at six geomagnetic stations
- Midlatitude stations register larger activity in solar cycles 15 and 16
- The difference depicts MLT dependence

Correspondence to:
D. Martini,
daniel.martini@oulu.fi

Citation:
Martini, D., K. Mursula, M. Orispää, and H.-J. Linthe (2015), Long-term decrease in the response of midlatitude stations to high-speed solar wind streams in 1914–2000, *J. Geophys. Res. Space Physics*, *120*, doi:10.1002/2014JA020813.

Received 12 NOV 2014
Accepted 17 MAR 2015
Accepted article online 21 MAR 2015

Long-term decrease in the response of midlatitude stations to high-speed solar wind streams in 1914–2000

D. Martini[1,2], K. Mursula[1], M. Orispää[3], and H.-J. Linthe[4]

[1]Space Physics Group, Department of Physics, University of Oulu, Oulu, Finland, [2]Norwegian Center for Space Weather, University of Tromsø, Tromsø, Norway, [3]Sodankylä Geophysical Observatory, University of Oulu, Oulu, Finland, [4]Adolf-Schmidt-Observatorium, GeoForschungsZentrum Potsdam, Niemegk, Germany

Abstract We investigate geomagnetic activity at two high-latitude, two midlatitude, and two low-latitude stations of the northern hemisphere and find that the increasing trend of geomagnetic activity in 1914–2000 is considerably lower at the two midlatitude stations (Niemegk and Fredericksburg) than at low- or high-latitude stations. As Niemegk occupies a specific position among geomagnetic stations, serving as the standard station for the *K/Ak* index derivation, it is crucial to understand the origin and long-term characteristics of this difference. We show here that geomagnetic activity at the studied midlatitude stations is relatively stronger in the declining phases of the 1 and 2 first solar cycles (15 and 16) than elsewhere, leading to the smaller long-term trend. We also find that the latitudinal differences in the trends are strongly dependent on local time, being considerably larger in the dawn sector. These differences can be explained by the relatively stronger contribution of high-speed streams to geomagnetic activity at the particular range of midlatitudes, compared to the stations at lower and higher latitudes.

1. Introduction

The interaction between the solar wind and the Earth's magnetosphere creates current systems in the magnetosphere and ionosphere that imprint their signal upon the ground-based magnetic measurements as irregular disturbances. These disturbances have been characterized by geomagnetic indices since the midnineteenth century, when continuous registering of Earth's magnetic field started [e.g., *Mayaud*, 1980, and references therein]. These index series are therefore the most widely used direct means to quantitatively study variations of the near-Earth space and solar activity at a century-long time scale. By averaging the time series of local indices from a number of stations, global indices have been formed that measure either specific current systems (e.g., the *AE*, *AU*, *AL*, and *Dst* indices) or the global disturbance level of geomagnetic activity (e.g., *aa*, *Kp*, and *Km*).

The local *K/Ak* indices [*Bartels et al.*, 1939] were originally hand derived from the analog records of one or more magnetic components at a given geomagnetic observatory. The range of the observed irregular variation in nanotesla is translated to an integer value between 0 and 9, the *K* value, in each 3 h interval. Geomagnetic activity is registered with largely different amplitudes in different magnetic latitudes, depending on the proximity of a given observatory to the major ionospheric-magnetospheric current systems. In order to allow quantitative interstation comparison from different observatories, at each observatory, a permanent scale is used to assign the *K* values to the range deviations, which scale is proportional to that defined at Niemegk [see also *Mayaud*, 1980; *Menvielle and Berthelier*, 1991]. Thus, the long-term probability distribution of *K* values at a particular station is normalized to that at Niemegk, making Niemegk the standard station in deriving all *K*-based indices.

The longest uniform global measure of geomagnetic activity, the *aa* index, is derived from the local *K* values of two antipodal observatory chains since 1868. One of the most important results of space climate science, the discovery of a notable increase of geomagnetic activity over the last century [*Mayaud*, 1972], was based on the long-term trend as registered by the *aa* index. Because of the unique length of the *aa* index series, the robustness and reliability of this index and its long-term trend are crucial in understanding the long-term evolution of near-Earth space and have been the subject of a long debate [*Stamper et al.*, 1999; *Lockwood et al.*, 1999; *Cliver and Ling*, 2002; *Svalgaard et al.*, 2004; *Mursula et al.*, 2004; *Jarvis*, 2005; *Mursula and Martini*,

Table 1. Information on Stations Used[a]

Station	IAGA Code	GG Lat	GG Long	GM Lat	MN
Sodankylä	SOD	67.47	26.60	63.96	22
Sitka	SIT	57.05	224.67	60.33	9
Niemegk	NGK	52.07	12.68	51.89	23
Fredericksburg	FRD	38.20	282.63	48.59	5
Tucson	TUC	32.25	249.17	40.06	7
Honolulu	HON	21.31	201.91	21.57	10

[a]Geographic latitude (GG lat) and geographic longitude (GG long) and geomagnetic latitude (GM lat); all in degrees. Magnetic coordinates are calculated using the International Geomagnetic Reference Field 2000 model. MN hour indicates the local midnight hour in UT.

2006; *Rouillard et al.*, 2007; *Svalgaard and Cliver*, 2007; *Love*, 2011; *Martini et al.*, 2012a; *Lockwood et al.*, 2013a], now favoring a minor multiplicative correction after 1957 [*Lockwood et al.*, 2014]. Unfortunately, the early records of magnetic observations that were used to construct the *aa* index are not available in digital format. Therefore, the exact digital reproduction of *aa* is impossible. These issues with the *aa* index have led to the introduction of a number of geomagnetic indices dedicated for long-term studies that are based on digitized hourly values, in particular the interhourly variability and interdiurnal variability indices [*Svalgaard et al.*, 2004; *Svalgaard and Cliver*, 2005], the *Ah* index [*Mursula and Martini*, 2006], the *AhK* index [*Martini et al.*, 2011], and the σ^H and *m* indices [*Finch et al.*, 2008; *Lockwood et al.*, 2013a].

When reanalyzing centennial geomagnetic activity using the digital *Ah* indices of six long operating stations, *Mursula and Martini* [2006, 2007] found that their trends vary greatly with latitude, with smallest increases found at the studied midlatitude stations. More recently, *Martini et al.* [2012a] standardized the indices, thus taking into account the different dispersion of the indices, and found that the latitudinal differences in the trends in 1901–2000 were considerably reduced. They also showed that the trend estimates are dependent on the time period studied [see also *Love*, 2011]. Notably, the two midlatitude stations, Niemegk and Fredericksburg, depicted a smaller increase in 1914–2000 than the stations at high and low latitudes, while the trends in 1901–2000 were to a large extent similar at all latitudes. Thus, not only the magnitude of the trend is interval dependent but so seems to be the relative trend difference between midlatitudes and other latitudes. Since the Niemegk station serves as reference for all other local and global *K*-based indices, it is essential to understand the origin and characteristics of this difference. In the present investigation, we will study the trends and their latitudinal differences in 1914–2000, paying special attention to the differences in trends in the different local time (LT) sectors. The paper is organized as follows. Sections 2 and 3 review the used index derivation method and the basic long-term characteristics of geomagnetic activity indices. Section 4 discusses the latitudinal differences of the six studied stations in 1914–2000. Section 5 focuses on the LT differences in the depicted long-term trends, while section 6 summarizes the main results and their implications.

2. Data and Method

We use data from the same six stations as in, e.g., *Martini et al.* [2012a] and *Mursula and Martini* [2006, 2007]. The stations are Sodankylä (SOD; Sodankylä Geophysical Observatory/University of Oulu) and Sitka (SIT) from high latitudes, Fredericksburg (FRD) and Niemegk (NGK; GFZ Potsdam) from midlatitudes, and Tucson (TUC) and Honolulu (HON) from low latitudes. (SIT, FRD, TUC, and HON are operated by U.S. Geological Survey). The geographic and geomagnetic coordinates of the stations together with their midnight UT times are shown in Table 1. These stations were originally selected on the basis that three latitude ranges are represented on an equal footing in this set (one pair for each region). Furthermore, these stations have the longest and most uniform magnetic records that make them especially suitable for long-term studies.

For the derivation of geomagnetic activity, we use the hourly mean *H* component data that are available from the World Data Center for Geomagnetism at Edinburgh. In this work, the *AhK* indices are used [*Martini et al.*, 2011] to quantify geomagnetic activity at each station. This method assigns eight *AhK* index values to each day as follows. First, the raw *H* data are run through a simple and robust recursive Kalman filter [*Kapio and Somersalo*, 2005] to estimate the regular magnetic variation (quiet daily curve (QDC)) for each day separately. Next, the amplitude of irregular activity, *AhK*, is defined in 3 h bins as the range difference (in nanotesla) between the upper and lower QDC envelopes fitted to the *H* data. The 3 h *AhK* values may be further averaged to obtain the daily or annual time series. As discussed earlier [*Mursula and Martini*, 2006], either *Ah* index method follows the derivation procedure of the traditional *K*/*Ak* index as closely as possible

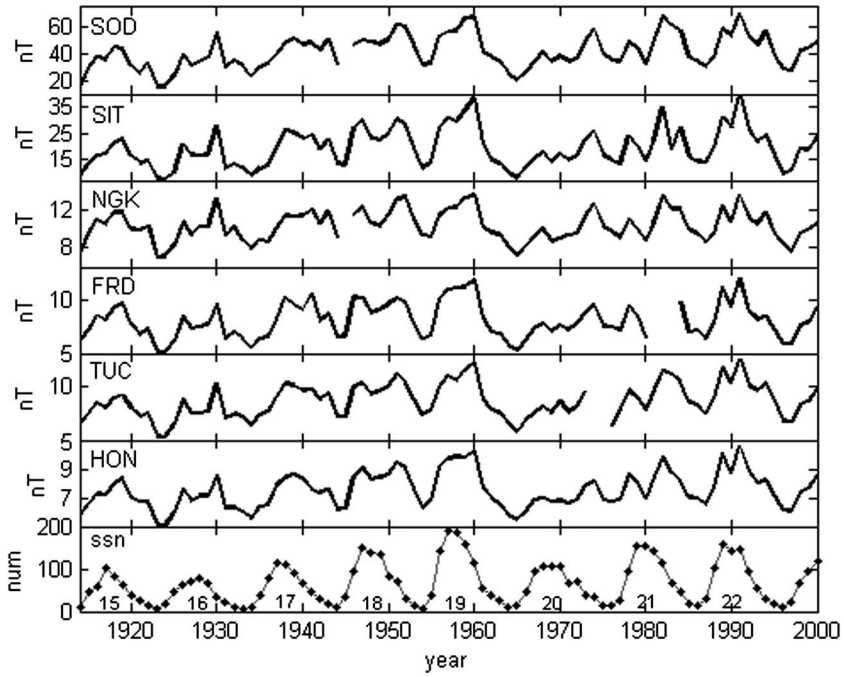

Figure 1. Time series of annual *AhK* indices of the six stations in 1914–2000. (bottom) The annual sunspot number with the corresponding cycle numbers is also shown for the same period.

for a digital index. It was also demonstrated [*Martini et al.*, 2011] that the Kalman method strongly improves the identification of QDC so that the resulting *AhK* index follows the well-known characteristics of local geomagnetic activity down to the highest 3 hourly sampling rate, better than the other studied digital indices based on hourly mean data.

3. Centennial Evolution of Geomagnetic Activity

Figure 1 depicts the annually averaged *AhK* indices of all six stations. Despite the fact that the indices are from different latitudes, the overall evolution of local geomagnetic activity is highly similar globally. Since observatories at different latitudes have different proximity to those major ionospheric/magnetospheric current systems channelling the solar wind energy, the scales of their disturbances, too, are bound to be different (see corresponding scales in Figure 1). Therefore, applying due normalization is essential for sensible interlatitude comparison. In the case of the traditional *K*/*Ak* index, such normalization is inherent in the *K* scaling, as discussed above. *Martini et al.* [2012a] used linear regression to NGK geomagnetic data and standardization (also called the *Z*-score method) to remove the effect of different absolute levels in the *AhK* series. They found that standardization provides more consistent results when considering different intervals. Therefore, the yearly *AhK* indices are standardized to the yearly AhK_Z indices by removing their mean (μ) over 1914–2000 and their standard deviation (σ) is used as unit measure about the mean:

$$AhK_Z = (AhK - \mu)/\sigma. \tag{1}$$

Thereafter, the probability density functions are similar, and a unit change in the standardized index represents the same relative change in the activity level at each station (analogously to the traditional *K*-based indices), allowing sensible interstation comparison.

3.1. On the Long-Term "Trend"

The characteristics of the evolution of geomagnetic activity in the twentieth century are well known by now [*Feynman and Crooker*, 1978; *Cliver and Ling*, 2002; *Mursula et al.*, 2004; *Mursula and Martini*, 2006; *Love*, 2011] and may be summarized as follows: on top of the solar cycle variation, with maxima following sunspot maxima with typically a few years lag, there is a clear upward drift of average activity level. It is, however,

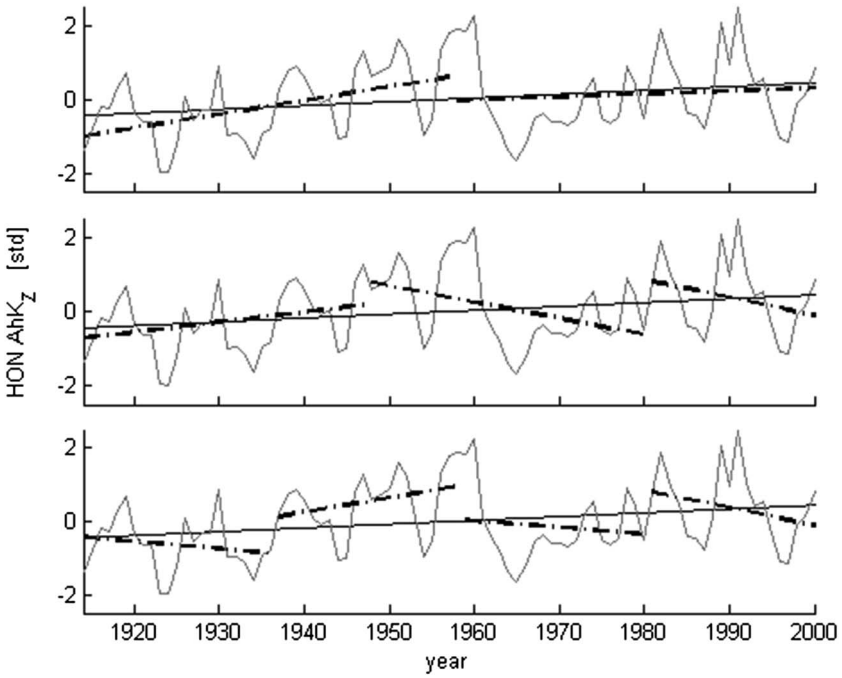

Figure 2. Comparisons of best fit lines to subset periods (dash-dotted line) of HON AhK_Z data in 1914–2000. The subset periods are defined as (top) 44, (middle) 33, and (bottom) 22 years, i.e., roughly 4, 3, and 2 solar cycle lengths, respectively. The length of the last period in each panel is the remaining fraction between the end of last full period and 2000. Note that while an increasing trend is obtained across the full interval (thin line), the depicted trends of subset periods are diverse.

important to note that this trend is far from linear or even monotonic. A larger increase takes place until solar cycle 19 (around early 1960s), which is followed by a dramatic drop of activity and a moderate increase thereafter until 2000.

One can check the steadiness of the linear trend by fitting subset periods of the data. Best fit lines to 22, 33, and 44 year long periods (roughly 2, 3, and 4 solar cycles, respectively) of HON AhK_Z series are shown in Figure 2. While there is an apparent increasing trend overall, fits to the subset periods are diverse. The interval concerned is thus a fundamental factor in the obtained magnitude of a trend estimate. Our definition of the long-term "trend" in geomagnetic activity is, therefore, the following: the average activity level is apparently larger in the last decades than in the first decades of the studied period of 1914–2000 [see also *Love*, 2011; *Martini et al.*, 2012a]. This apparent drift gave motivation for quantifying the secular change of geomagnetic activity by estimating the linear trend [e.g., *Feynman and Crooker*, 1978; *Lockwood et al.*, 1999; *Mursula et al.*, 2004; *Mursula and Martini*, 2006, 2007; *Martini et al.*, 2012a]. Because of valid concern of whether the observations are best characterized by a simple linear trend (and thus by the slope), we also look into the percentage change between the mean values during the first versus last 22 years (roughly two solar cycles). The percentage change depends only on the beginning and end values; it is therefore independent from the midcentury development and does not require the assumption of linearity [see also *Martini et al.*, 2012a, and references therein]. Note also that, due to the chosen period of 1914–2000, our time series run from near solar minimum to near maximum. Our analysis shows that limiting the study to, e.g., solar cycles 15–22 and thus quantifying the evolution from solar minimum to minimum would lead to virtually identical long-term patterns to those discussed below (not shown).

4. Latitudinal Differences of Geomagnetic Indices

Figure 3 depicts the six AhK_Z series, together with the corresponding best fit lines using ordinary least squares algorithm. The long-term trends, estimated by the slope of the best fit line and the percentage change for each AhK_Z series, are included in Table 2. It is clear that while indices from high and low latitudes have roughly the same larger slope over the selected interval (about 0.010–0.013), both the two midlatitude stations of NGK and FRD have considerably smaller slopes (about 0.003–0.004); also, the corresponding average increase

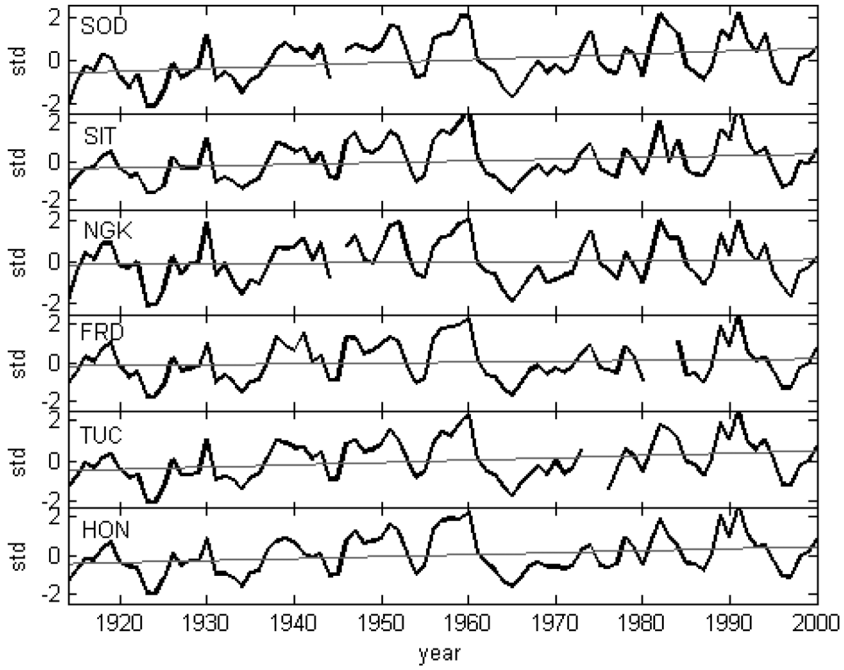

Figure 3. Time series of the annual standardized AhK_Z indices of the six stations in 1914–2000. The units are in respective standard deviation. The best fit line is also depicted for each station (for the corresponding slope, as well as the percentage change of the mean values in the first/last 22 years, see Table 2).

of NGK and FRD in 1914–2000 is about 20%, which is only about half of the increase found at either high or low latitudes [see also *Martini et al.*, 2012a].

One could look into the error of the slopes to determine if the midlatitude difference is significant. A simple error analysis, however, would render the regular (solar cycle related) cyclical pattern as random dispersion, giving a false estimate on the uncertainty. We therefore choose to calculate the 11 year running mean of the AhK_Z series that considerably reduces the cyclicity of the data. The regression analysis is carried out on this running mean data at each station. The procedure is shown in Figure 4 for SOD. The obtained slopes and their standard errors (assuming normal distribution) are listed in Table 2. Note that the first and last years are omitted from this analysis. The reduced interval inevitably leads to a somewhat larger scatter in the obtained slopes, S_{rm}, but the trends at NGK and FRD remain clearly smaller than at the other stations. While uncertainties are large, one can say at this point with 90% confidence ($P = 0.1$) that some of the latitudinal differences, between either midlatitude station versus SOD or TUC in particular, are real. The rather systematic behavior indicates that the apparent latitudinal difference could carry physical meaning. The above-mentioned fact that NGK serves as a reference station in *K* index derivation makes this peculiar disparity especially important. Therefore, we focus our study to NGK data with the important remark that the smaller trend estimate is highly similar at FRD, indicating a global pattern.

Table 2. The Annual Increase (Slope) of Best Fit Line to the Standardized Ahk_z Index and the Relative Change in Percent Between the Ahk_z Means in the First and Last 22 Years in 1914–2000[a]

Station	Slope (σ/yr)	% Change	S_{rm} (σ/yr)	SE of S_{rm}
SOD	0.013	53	0.016	0.0028
SIT	0.010	38	0.010	0.0025
NGK	0.004	18	0.007	0.0022
FRD	0.003	22	0.008	0.0024
TUC	0.012	50	0.016	0.0029
HON	0.010	44	0.012	0.0027

[a]For the error analysis, the slope (S_{rm}) of best fit line to the 11 year running mean values of AhK_Z and its error (SE) for each station is also listed.

To study the relative drifts in more detail, one can analyze the differences between the stations. Figure 5 depicts the differences between two pairs of high- and low-latitude stations and Figure 6 between NGK and high- and low-latitude station. While the differences between the high- and low-latitude indices (Figure 5) depict random scatter around zero over the studied period, indicating that these indices register essentially the same

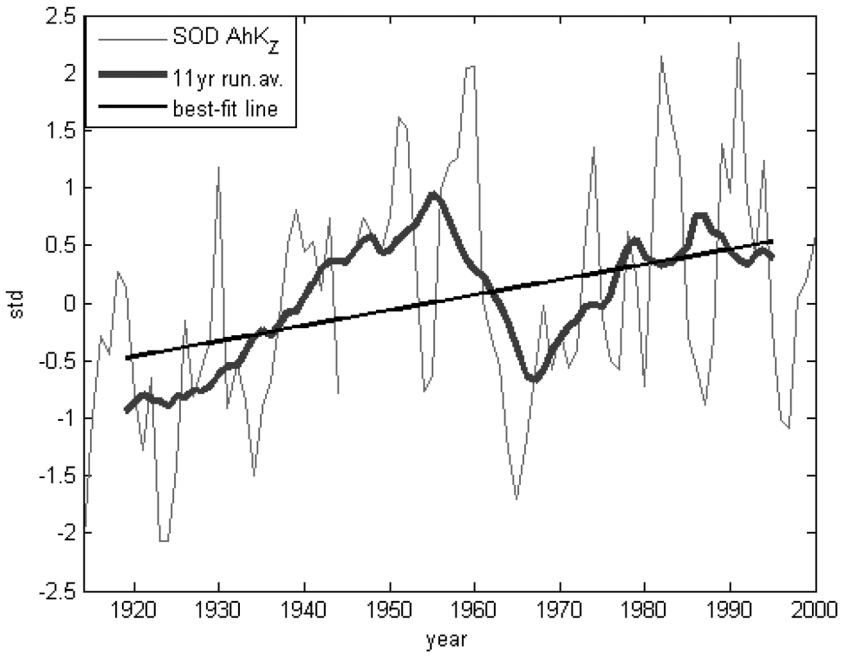

Figure 4. The annual indices (thin line) and the 11 year running means (thick curve) of SOD AhK_Z and the best fit line to running mean data (in 1919–1995, inclusive).

long-term variation, it is clear that the differences between NGK and other stations (Figure 6) exhibit a different, systematic pattern. The differences depicted in Figure 6 have two components: (i) a solar cycle-dependent oscillation, which is particularly large in NGK-HON difference, and a (ii) long-term drift. We will study these two components separately.

4.1. Solar Cycle Variation in Trend Difference

Geomagnetic activity is primarily driven by two major types of solar wind structures: the coronal mass ejections (CME) and the high-speed streams (HSSs) in association with corotating interaction regions. The CMEs dominate during years of peak solar activity, while HSSs are mainly emitted from the equatorward expanding solar polar coronal holes during the declining solar cycle phase [*Richardson et al.*, 2000; *Richardson and Cane*, 2012]. It is known that CMEs and HSSs drive geomagnetic activity differently. The strong geoeffectiveness of CMEs causing large magnetic disturbances primarily depends on the sustained presence of southward component of interplanetary magnetic field (IMF), B_z, while HSSs also affect via the higher mean solar wind speed (V) [*Tsurutani et al.*, 2006; *Finch et al.*, 2008]. Note also that, although it is the southward component that principally drives geomagnetic activity, on annual time scales, the IMF orientation averages such that disturbances are essentially controlled by the IMF strength, $B = |\,|\vec{B}\,|\,|$ [*Stamper et al.*, 1999].

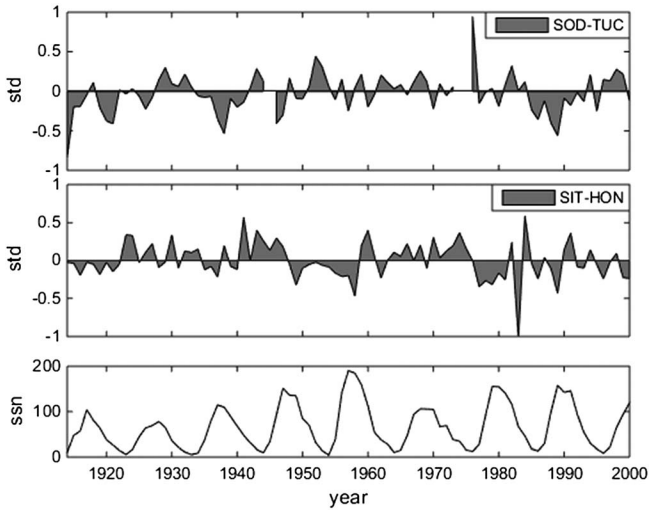

Figure 5. Differences between the annual AhK_Z indices in 1914–2000: (top) SOD-TUC and (bottom) SIT-HON. (Figure 5, bottom) Annual sunspot numbers are included for the same period (thin line).

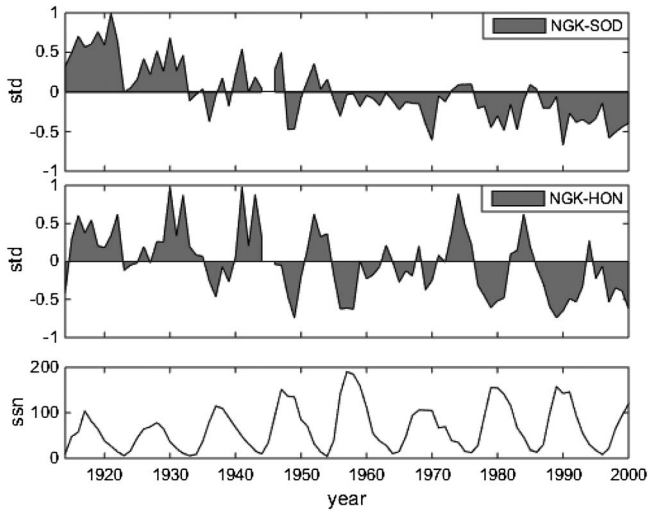

Figure 6. Differences of annual AhK_Z indices in 1914–2000: (top) NGK-SOD and (bottom) NGK-HON. (Figure 6, bottom) Annual sunspot numbers are included for the same period in (thin line).

Table 3 shows the zero lag Pearson correlation coefficients between the annual AhK_Z indices and the single parameter coupling functions of *V* and *B* in 1965–2000. At all stations, the correlation coefficients are larger for *B* than for *V*, which we interpret as indicating that the AhK_Z index is predominantly driven by *B* rather than *V*. This is in agreement with earlier results [*Svalgaard and Cliver*, 2007; *Finch et al.*, 2008; *Martini et al.*, 2012b; *Lockwood et al.*, 2013b], showing that indices derived from hourly mean data have a somewhat damped response to high-frequency fluctuations driven by Alfvén waves in high-speed streams due to the smoothing effect of hourly averaging. Note that NGK has the strongest coupling to *V* and, in turn, the weakest coupling to *B*. It has even a stronger correlation with *V* than the auroral SOD station (note that typically auroral stations have stronger correlation with *V* than stations at other latitudes [*Finch et al.*, 2008; *Holappa et al.*, 2014]).

Table 3 helps in identifying the likely origin of the solar cycle oscillation of the differences in Figure 6. When geomagnetic disturbances are dominated by HSSs in the declining solar cycle phase, NGK, due to its stronger dependence on *V*, registers somewhat higher AhK_Z than most other stations. On the other hand, when disturbances are directly driven by CMEs around solar maxima, NGK, due to its weaker dependence on *B*, registers suppressed AhK_Z. This is in agreement with recent results of *Holappa et al.* [2014], where it was demonstrated that the fraction of HSS (CME)-related activity in annual geomagnetic activity depicts a local maximum (minimum, respectively) at the specific range of midlatitudes where NGK is situated. The different dependence to HSSs versus CMEs was also held accountable for the dominant fraction of observed differences in geomagnetic activity between the geomagnetic stations. The enhanced sensitivity to *V* at NGK and the somewhat weaker association with *B* also straightforwardly explains the cyclic pattern in the differences depicted in Figure 6.

4.2. Long-Term Drift in Trend Difference

We define the annual occurrence counts of geomagnetically active days (quiet days) as the number of daily *AhK* values per year in the upper (lower, respectively) quartile, i.e., values occupying the upper/lower 25% of the total probability density function. These two yearly occurrence counts in 1914–2000 are depicted in Figure 7 for SIT, NGK, and HON stations. One can see that the increase of geomagnetically active days is associated with the corresponding decrease of quiet days at each station. This is expected as the two quartiles represent the two opposite tails of the probability density function.

Table 3. Pearson Correlation Coefficients (Cc) at Zero Lag Between the Annual Ahk_z and Solar Wind Speed *V* and IHM Strength *B* in 1965–2000[a]

Station	*B*	*V*
SOD	0.81	0.65
SIT	0.85	0.53
NGK	0.77	0.70
FRD	0.85	0.52
TUC	0.86	0.57
HON	0.90	0.45

[a]All coefficients are significant with $P < 0.01$.

We quantify the apparent long-term change in Figure 7 by the cumulative exceedance counts (i.e., the cumulative sums of annual counts within the specific periods defined below) and slopes of the best fit line to exceedances, whose value (in number of days per year) is also depicted in Figure 7. The best fit line slopes show that NGK depicts by far the smallest increase in active days, only 0.12 d/yr.

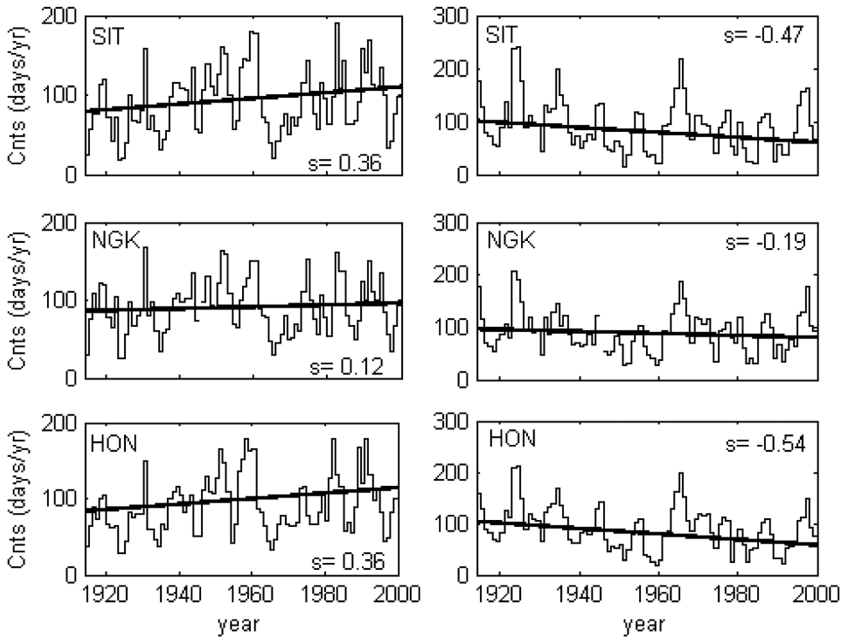

Figure 7. (left (right)) Annual occurrence count rates of upper (lower, respectively) quartile values of *AhK* for (top) SIT, (middle) NGK, and (bottom) HON in 1914–2000. The slopes of the best fitting linear trends in 1914–2000 are also indicated.

(Note that the corresponding slope at FRD is 0.11 d/yr, i.e., very close to that of NGK; not shown). In order to demonstrate the underlying physical differences in station responses, we analyze in more detail the period of 1914–1960, where the (increasing or decreasing) trend in Figure 7 is to a large extent persistent [*Cliver and Ling*, 2002]. As discussed above (see Figure 6), the most prominent differences occur in the declining phases. At NGK, one finds, e.g., a cycle maximum of 119 active days in 1919, 169 in 1930, and 151 in 1960, in the declining phases of cycles 15, 16, and 19. These values compare to 120/159/179 in 1919/1930/1959 at SIT and 105/149/179 at HON in 1919/1930/1958. Curiously, in cycle 19, when the highest maximum of active days takes place at all other stations, NGK depicts a relatively low maximum, lower than in cycles 16 and 18. The relative overestimate of active days in early decades (cycles 15 and 16) and the underestimate in the 1960s contribute to a lower long-term trend at NGK (both in the number of active days, Figure 7, and overall geomagnetic activity, Figure 6). The cumulative exceedances are 1469 for SIT, 1732 for NGK, and 1496 for HON in 1914–1936 while 2243/2076/2276 in 1979–2000. These correspond to 53% (52%) increase at SIT (HON, respectively) that compares to a 19% increase at NGK. Thus, the same pattern of considerably lower midlatitude increase is observed. Note that these percentage increases of cumulative exceedance counts at all three stations are very close to those obtained for the AhK_Z series (see Table 2).

Note also that the decrease in the number of quiet days in 1914–2000 is more rapid than the corresponding increase in active days at all stations. This is in agreement with previous suggestions based on the *K* and *aa* indices that the increasing activity during relatively quiet years is an important factor of the overall centennial increase, besides the increasing occurrence of magnetic storms [*Feynman and Crooker*, 1978; *Vennerstroem*, 2000; *Love*, 2011].

Figure 8 repeats the relative drift between NGK and SOD in 1914–2000 and depicts the similar relative drift between FRD and SOD. The dominant common feature is the large decreasing trend in both differences over this time interval. However, the cycle variation of FRD-SOD difference is quite different from the NGK-SOD difference. While both differences attain large positive values in the declining phase of cycles 15 and 17, the AhK_Z values are larger at SOD than FRD during the declining phases of all other cycles, while the NGK-SOD differences remain positive until the declining phase of cycle 21. Thus, the underlying common cause to the long-term drift of the two differences of Figure 8 is the decreasing sensitivity of the two midlatitude stations to HSSs relative to SOD, which proceeds slightly faster at FRD than at NGK. Note also that, as shown in Table 2, FRD has a much weaker coupling to *V* in 1965–2000 than SOD (unlike NGK), as shown by consistently negative values of the FRD-SOD difference in the declining phases of cycles 20–22 (see Figure 8).

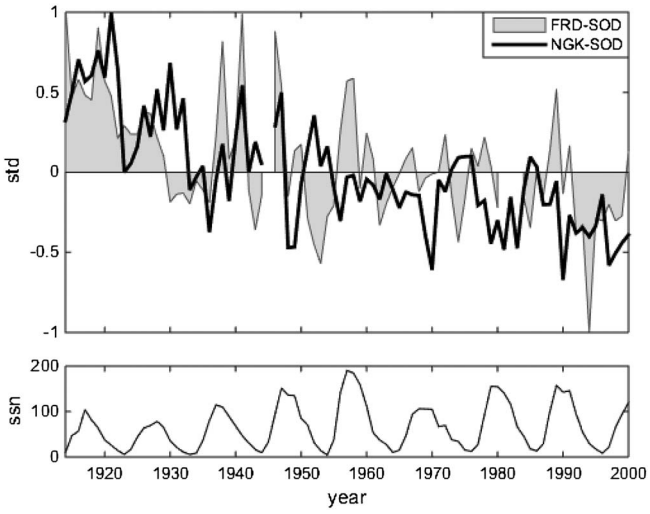

Figure 8. Differences of the annual AhK_Z indices for NGK-SOD (thick line) and FRD-SOD (thin line and shaded area) in 1914–2000. (bottom) Annual sunspot numbers are included for the same period(thin line).

5. LT Dependence

5.1. LT Dependence of Trend Differences

High-speed streams control substorm occurrence and most of geomagnetic activity at annual time scales [*Tanskanen et al.*, 2005; *Hwang et al.*, 2008; *Holappa et al.*, 2014]. Since substorms form the substorm current wedge and increase the westward electrojet in the auroral ionosphere [e.g., *Kamide*, 1995], which maximizes in the midnight-dawn LT sector, one would expect to find differences in the long-term trends in the different LT sectors. We therefore define eight new magnetic indices, AhK_i ($i = 1{:}8$), where each 3 h UT bin is treated separately to form eight annually averaged series. As final step, all eight sets are standardized to form AhK_{Zi}. The advantage of this formulation is that the eight UT (or LT, correspondingly) bins allow studying the diurnal variation of the trends.

Direct interstation comparison of the AhK_{Zi} indices is somewhat problematic because the 3 hourly UT sections often correspond to different LT hours at the different stations. NGK and SOD are both located in the European sector with only 1 h difference (NGK LT(h) = UT(h) + 1 h; SOD LT(h) = UT(h) + 2 h), thus mostly overlapping in LT. We note that the 1 h LT difference does not produce significant differences in their statistical properties [see also *Martini et al.*, 2012b].

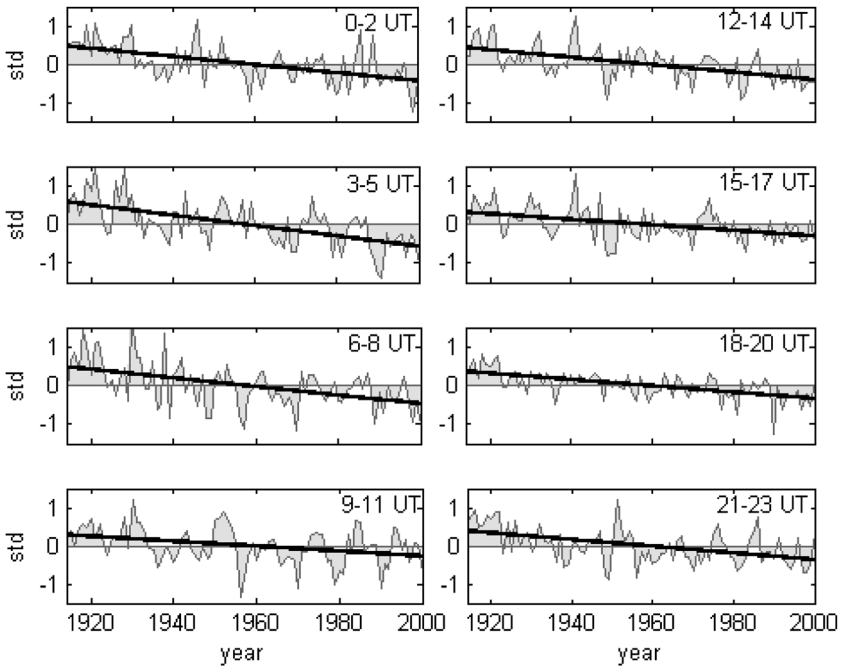

Figure 9. Differences AhK_{Zi} (NGK)-AhK_{Zi} (SOD) for the eight 3 hourly UT sectors with best fit lines in 1914–2000. The corresponding slopes, percentage changes, and variances are listed in Table 4, while the slopes and variances are also conjointly depicted in Figure 9 as function of NGK LT.

Table 4. Slopes, Percentage Changes Between Mean Values of the First/Last 22 Years, Variances (σ^2), and Their RMS Errors for the NGK-SOD AhK_{Zi} Differences in the Eight UT Bins[a]

	00:00–02:00 UT	03:00–05:00 UT	06:00–08:00 UT	09:00–11:00 UT	12:00–14:00 UT	15:00–17:00 UT	18:00–20:00 UT	21:00–23:00 UT
Slope (σ/yr)	0.0106	0.0134	0.0111	0.0065	0.0098	0.0072	0.0081	0.0088
% change	−21	−28	−22	−15	−20	−16	−17	−18
σ^2	0.236	0.316	0.330	0.236	0.193	0.167	0.119	0.214
RMS error of σ^2	0.036	0.050	0.050	0.036	0.029	0.025	0.018	0.033

[a]Note that NGK UT(h) = LT(h) − 1(h).

The NGK-SOD differences from the eight AhK_{Zi} indices in 1914–2000 are depicted in Figure 9. The dominant feature in Figure 9 is the substantial excess of NGK AhK_{Zi} levels leading to positive NGK-SOD differences around the declining phases of cycles 15 and 16 (also cycle 17 in the afternoon sector) that maximize in the dawn-to-morning sector (03:00–08:00 UT), but remain apparent in all but the dusk-night sector (18:00–23:00 UT), where large NGK AhK_{Zi} values are found only in cycle 15. This excess activity level at NGK is the dominant contributor to the observed long-term drift between the stations. The largest differences thus arise in the declining phases of the early cycles 15 and 16, when HSS activity (presumably) dominates especially in the dawn-morning sector that is most favorable for registering substorm-related geomagnetic activity (that is, in turn, strongly modulated by HSSs). Lastly, let us note that the most regular solar cycle-dependent oscillation with the smallest relative drift between the two stations is found in the prenoon sector (09:00–11:00 UT), with NGK being consistently larger (smaller) in the declining phase (solar maximum, respectively). This is in agreement with above discussion of NGK's stronger dependence on V (Table 3).

We use different approaches to quantify the properties of the differences depicted in Figure 9: (i) the slope of the best fit line and the percentage change (as above) and (ii) the variance, σ^2, of the differences in each UT bin. While variance quantifies the dispersion of differences, the slope and percentage change gives information about possible relative long-term drifts. The slopes, percentages, and variances of the NGK-SOD differences are listed in Table 4. The slopes and variances are also conjointly displayed in Figure 10 in NGK LT. As seen in Figure 10, the variance in the NGK-SOD differences depicts a continuous daily evolution with the smallest value of $\sigma^2 = 0.119$ in the dusk sector (18:00–20:00 UT, central LT at about 20 h). It is followed by a steady increase until the dawn/early morning side, where it reaches its maximum ($\sigma^2 = 0.330$; 06:00–08:00 UT, central LT at about 8 h), almost 3 times the variance in the dusk. Note that this LT evolution of variances is significant at a 3–4 sigma level (see Table 4). Similarly, the magnitudes of slopes and the percentage changes that carry the information about the long-term drift between the stations, also maximize in the dawn sector (03:00–05:00 UT, central LT at about 5 h) and are small in the evening-premidnight sector. The smallest trend is found on the dayside (09:00–11:00 UT). It is thus clear that as discussed above, the dominant part of the difference between NGK and SOD originates in the early morning sector, where the westward electrojet dominates the activity. In contrast, both the drift and variance are highly reduced in the dusk sector (18:00–20:00 UT), where the directly driven process is dominant [*Finch et al.*, 2008].

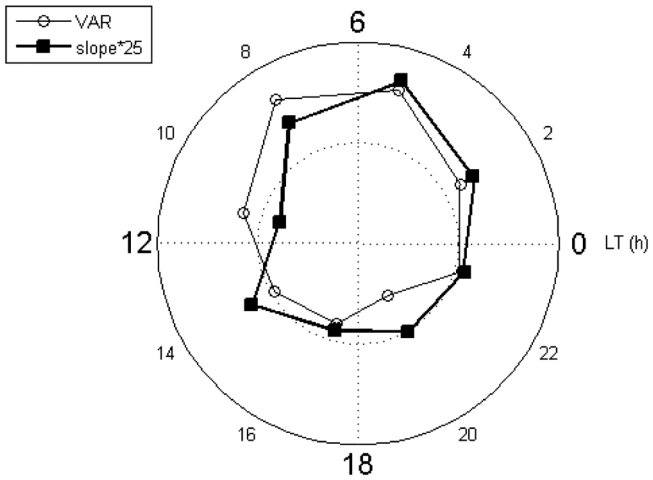

Figure 10. LT dependence of the variances (VAR = σ^2) of and the magnitudes of slopes of the differences of AhK_{Zi} indices between NGK and SOD in 1914–2000. The 3 hourly UT intervals are located at the central hour of NGK LT(h) = UT(h) + 1(h). The solid (dotted) circle corresponds to 0.4 (0.2). (Slopes are multiplied by 25.)

Due to the geographic position of FRD observatory, the only station with overlapping LT sector is the low-latitude TUC station (see Table 1). Therefore, we study the FRD-TUC sector differences in the eight LT sectors. Note, however, that the stations differ by 2 LT hours,

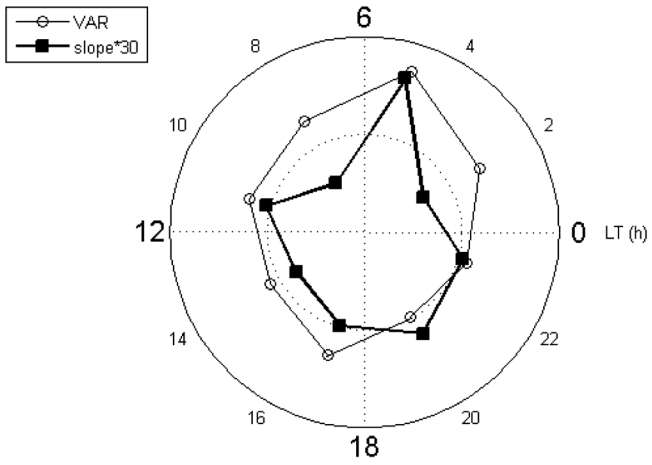

Figure 11. Same as in Figure 8 for FRD-TUC difference. The 3 hourly UT intervals are located at the central hour of FRD LT(h) = UT(h) − 5(h). (Slopes are multiplied by 30.)

which possibly brings some inherent inaccuracy to this comparison. The slopes and variances for FRD-TUC sector differences are plotted (using FRD LT) in Figure 11 and listed (with percentages and the corresponding root-mean-square (RMS) errors of variance) in Table 5. Although the LT dependence of variance is more isotropic (presumably due to the longer interstation LT difference), it is significant and follows a similar pattern as that of NGK-SOD, being smallest around dusk (LT = 20 h) and largest in the dawn sector (LT = 5 h). Similarly, we find that the magnitude of relative drift between FRD and TUC is most pronounced in the dawn sector (LT = 5 h).

6. Discussion and Conclusions

We have studied differences in the long-term trend estimates of geomagnetic activity indices derived from hourly mean data in 1914–2000. It was earlier shown [*Love*, 2011; *Martini et al.*, 2012a] that such differences are dependent on the interval studied. While the trends at different latitudes remain roughly similar in 1901–2000, the midlatitude NGK and FRD stations depict less than half the increase in 1914–2000 than found at high and low latitudes.

In the declining phases of cycles 15–16, when geomagnetic activity was dominated by recurrent high-speed solar wind streams [*Mursula et al.*, 2015], NGK and FRD depict mostly larger activity than other stations. This contributes to the obtained smaller trends in 1914–2000 at these two stations. We have shown that this difference has a clear local time dependence, being largest in the dawn and smallest in the dusk sector. Thus, the difference is most apparent at those local times where the effect of substorms, reflecting the high-speed stream solar wind structures, typically dominates geomagnetic activity. While uncertainties in some of the trend estimates are large, the used methods give strong support for a substantial difference in the long-term geomagnetic activity at NGK and FRD; the systematic behavior of these midlatitude stations against both higher- and lower-latitude stations indicates a global pattern.

Our results are further supported by recent report on the long-term difference in geomagnetic response to solar wind drivers at the midlatitudes. As shown in Figure 8, the sensitivity to high-speed stream-driven variations seems to have been consistently decreasing in 1914–2000 at both studied midlatitude stations, faster at FRD than at NGK. *Holappa et al.* [2014] find the different relative sensitivity to CME- and HSS-related activity to be the dominant factor in the spatial (latitudinal) differences of geomagnetic activity at the different stations. Long-term changes in the stations' relative position with respect to activity source regions could therefore be responsible for the observed gradual change in NGK and FRD magnetic field sensitivity to HSS-related geomagnetic variations. The secular change of the Earth's magnetic field may drive this change in relative geometry.

Table 5. Slopes, Percentage Changes Between Mean Values of the First/Last 22 Years, Variances (Σ^2), and Their RMS Errors From FRD-TUC Ahk_{zi} Differences in the Eight UT Bins[a]

	00:00–02:00 UT	03:00–05:00 UT	06:00–08:00 UT	09:00–11:00 UT	12:00–14:00 UT	15:00–17:00 UT	18:00–20:00 UT	21:00–23:00 UT
Slope (σ/yr)	0.0080	0.0070	0.0047	0.0109	0.0039	0.0070	0.0054	0.0066
% change	−20	−20	−13	−26	−14	−19	−15	−17
σ^2	0.199	0.220	0.270	0.342	0.259	0.247	0.222	0.263
RMS error of σ^2	0.030	0.034	0.041	0.052	0.040	0.038	0.034	0.040

[a]Note that FRD UT(h) = LT(h) + 5(h).

Global geomagnetic indices (like *Kp*, *Ap*, and *aa*) have been derived in some cases since the nineteenth century and include recordings stretching over a wide latitude and/or local time range. It is important to understand that the individual stations of these composites may have quite different responses to solar wind drivers; therefore, the interpretation of their characteristics, such as their long-term trend, is not at all straightforward. To address the question to what extent, if at all, these differences affect global indices where NGK data serves as reference (such as, e.g., the traditional *K*-based indices) is left for future studies.

Acknowledgments

We thank the staff of geomagnetic observatories and data archives whose consistent work has made this long-term study possible. The hourly magnetometer data were obtained from the World Data Center for Geomagnetism, Edinburgh (http://www.wdc.bgs.ac.uk); sunspot data were obtained from WDC-SILSO, Royal Observatory of Belgium, Brussels (http://sidc.be/silso); and the (Earth-shifted) hourly values of solar wind and IMF were obtained from the OMNI database (http://omniweb.gsfc.nasa.gov). The derived data (the *AhK*, AhK_Z, and AhK_{Zi} indices) can be obtained from D. Martini (Daniel.Martini@oulu.fi) upon request. We acknowledge the financial support by the Academy of Finland to the ReSoLVE Centre of Excellence (project 272157). This work has also benefited from collaborations and contacts within the COST ES1005 (TOSCA) Network Action (esp. Working Group 2).

Yuming Wang thanks the reviewers for their assistance in evaluating this paper.

References

Bartels, J., N. H. Heck, and H. F. Johnston (1939), The three-hour range index measuring geomagnetic activity, *J. Geophys. Res.*, *44*, 411–454, doi:10.1029/TE044i004p00411.

Cliver, E. W., and A. G. Ling (2002), Secular change in geomagnetic indices and the solar open magnetic flux during the first half of the twentieth century, *J. Geophys. Res.*, *107*(A10), 1303, doi:10.1029/2001JA000505.

Feynman, J., and N. U. Crooker (1978), The solar wind at the turn of the century, *Nature*, *275*, 626–627.

Finch, I. D., M. L. Lockwood, and A. P. Rouillard (2008), Effects of solar wind magnetosphere coupling recorded at different geomagnetic latitudes: Separation of directly driven and storage/release systems, *Geophys. Res. Lett*, *35*, L21105, doi:10.1029/2008GL035399.

Holappa, L., K. Mursula, T. Asikainen, and I. G. Richardson (2014), Annual fractions of high speed streams from principal component analysis of local geomagnetic activity, *J. Geophys. Res. Space Physics*, *119*, 4544–4555, doi:10.1002/2014JA019958.

Hwang, J., K.-H. Kim, K.-S. Cho, and Y.-D. Park (2008), Analysis of the correlations between the occurrence of substorm injections and interplanetary parameters during declining phase of solar cycle 23, *J. Korean Phys. Soc.*, *53*(2), doi:10.3938/jkps.53.897.

Jarvis, M. J. (2005), Observed tidal variation in the lower thermosphere through the 20th century and the possible implication of ozone depletion, *J. Geophys. Res.*, *110*, A04303, doi:10.1029/2004JA010921.

Kamide, Y. (1995), Aurora/substorm studies with incoherent scatter radars, Incoherent scatter-Tech. Rep. 97/53, EISCAT Scientific Association.

Kapio, J., and E. Somersalo (2005), *Statistical and Computational Inverse Problems*, Springer, New York.

Lockwood, M., R. Stamper, and M. N. Wild (1999), A doubling of the Sun's coronal magnetic field during the past 100 years, *Nature*, *399*, 437–439, doi:10.1038/20867.

Lockwood, M., L. Barnard, H. Nevanlinna, M. J. Owens, R. G. Harrison, A. P. Rouillard, and C. J. Davis (2013a), Reconstruction of geomagnetic activity and near-Earth interplanetary conditions over the past 167 years: Part 1. A new geomagnetic data composite, *Ann. Geophys.*, *31*, 1957–1977, doi:10.5194/angeo-31-1957-2013.

Lockwood, M., L. Barnard, H. Nevanlinna, M. J. Owens, R. G. Harrison, A. P. Rouillard, and C. J. Davis (2013b), Reconstruction of geomagnetic activity and near-Earth interplanetary conditions over the past 167 years: Part 2. A new reconstruction of the interplanetary magnetic field, *Ann. Geophys.*, *31*, 1979–1992, doi:10.5194/angeo-31-1979-2013.

Lockwood, M., H. Nevanlinna, L. Barnard, M. J. Owens, R. G. Harrison, A. P. Rouillard, and C. J. Scott (2014), Reconstruction of geomagnetic activity and near-Earth interplanetary conditions over the past 167 years: Part 4. Near-Earth solar wind speed, IMF, and open solar flux, *Ann. Geophys.*, *32*, 383–399, doi:10.5194/angeo-32-383-2014.

Love, J. J. (2011), Secular trends in storm level geomagnetic activity, *Ann. Geophys.*, *29*, 251–262, doi:10.5194/angeo-29-251-2011.

Martini, D., M. Orispää, T. Ulich, M. Lehtinen, K. Mursula, and D.-H. Lee (2011), Kalman filter technique for defining solar regular geomagnetic variations: Comparison of analog and digital methods at Sodankylä observatory, *J. Geophys. Res.*, *116*, A06102, doi:10.1029/2010JA016343.

Martini, D., H. J. Linthe, V. S. Pandey, and D.-H. Lee (2012a), On the centennial trend estimates of geomagnetic activity indices, *J. Geophys. Res.*, *117*, A06211, doi:10.1029/2012JA017564.

Martini, D., K. Mursula, T. Ulich, V. S. Pandey, K.-H. Kim, and D.-H. Lee (2012b), Long-term changes in indices of geomagnetic activity at the auroral station Sodankylä, *J. Adv. Space Res.*, *50*(6), 690–699, doi:10.1016/j.asr.2012.01.013.

Mayaud, P.-N. (1972), The *aa* indices: A 100 year series characterizing the magnetic activity, *J. Geophys. Res.*, *77*(34), 6870–6874, doi:10.1029/JA077i034p06870.

Mayaud, P.-N. (1980), *Derivation, Meaning, and Use of Geomagnetic Indices*, *Geophys. Monogr. Ser.*, vol. 22, 154 pp., AGU, Washington D. C., doi:10.1029/GM022.

Menvielle, M., and A. Berthelier (1991), The *K*-derived planetary indices: Description and availability, *Rev. Geophys.*, *29*(3), 415–432.

Mursula, K., and D. Martini (2006), Centennial increase in geomagnetic activity: Latitudinal differences and global estimates, *J. Geophys. Res.*, *111*, A08209, doi:10.1029/2005JA011549.

Mursula, K., and D. Martini (2007), A new verifyable measure of centennial geomagnetic activity: Modifying the *K* index method for hourly data, *Geophys. Res. Lett.*, 34, L22107, doi:10.1029/2007GL031123.

Mursula, K., D. Martini, and A. Karinen (2004), Did open solar magnetic field increase during the last 100 years? A reanalysis of geomagnetic activity, *Sol. Phys.*, *224*, 85–94.

Mursula, K., R. Lukianova, and L. Holappa (2015), Occurrence of high-speed solar wind streams over the Grand Modern Maximum, *Astrophys. J.*, 801, *30*, doi:10.1088/0004-637X/801/1/30.

Richardson, I. G., and H. V. Cane (2012), Near-Earth solar wind flows and related geomagnetic activity during more than four solar cycles (1963–2011), *J. Space Weather Space Clim.*, *2*, A02, doi:10.1051/swsc/2012003.

Richardson, I. G., E. W. Cliver, and H. V. Cane (2000), Sources of geomagnetic activity over the solar cycle: Relative importance of coronal mass ejections, high-speed streams, and slow solar wind, *J. Geophys. Res.*, *105*, 18,203–18,214, doi:10.1029/1999JA000400.

Rouillard, A. P., M. Lockwood, and I. Finch (2007), Centennial changes in the solar wind speed and open solar magnetic flux, *J. Geophys. Res.*, *112*, A05103, doi:10.1029/2006JA012130.

Stamper, R., M. Lockwood, M. Wild, and T. Clark (1999), Solar causes of the long-term increase in geomagnetic activity, *J. Geophys. Res.*, *104*, 28,325–28,342, doi:10.1029/1999JA900311.

Svalgaard, L., and E. W. Cliver (2005), The IDV index: Its derivation, use in inferring long-term interplanetary magnetic field strength, *J. Geophys. Res.*, *110*, A12103, doi:10.1029/2005JA011203.

Svalgaard, L., and E. W. Cliver (2007), Interhourly variability index of geomagnetic activity and its use in deriving the long-term variation of solar wind speed, *J. Geophys. Res.*, *112*, A10111, doi:10.1029/2007JA012437.

Svalgaard, L., E. W. Cliver, and P. Le Sager (2004), IHV, a new long-term geomagnetic index, *Adv. Space Res.*, *34*, 436–439, doi:10.1016/j.asr.2003.01.029.

Tanskanen, E. I., J. A. Slavin, A. J. Tanskanen, A. Viljanen, T. I. Pulkkinen, H. E. J. Koskinen, A. Pulkkinen, and J. Eastwood (2005), Magnetospheric substorms are roughly modulated by interplanetary high-speed streams, *Geophys. Res. Lett.*, *32*, L16104, doi:10.1029/2005GL023318.

Tsurutani, B. T., et al. (2006), Corotating solar wind streams and recurrent geomagnetic activity: A review, *J. Geophys. Res.*, *111*, A07S01, doi:10.1029/2005JA011273.

Vennerstroem, S. (2000), Long-term rise in geomagnetic activity: A close connection between quiet days and storms, *Geophys. Res. Lett.*, *27*, 69–72, doi:10.1029/1999GL010727.